Mechanism of Spinach Chloroplast Ferredoxin-Dependent Nitrite Reductase: Spectroscopic Evidence for Intermediate States†

Sofya Kuznetsova,‡ David B. Knaff,§,|| Masakazu Hirasawa,§ Bernard Lagoutte,‡ and Pierre Sétif*,‡

Service de Bioénergétique and CNRS URA 2096, Département de Biologie Joliot Curie, CEA Saclay, 91191 Gif-sur-Yvette Cedex, France, and Department of Chemistry and Biochemistry and Center for Biotechnology and Genomics, Texas Tech University, Lubbock, Texas 79409-1061

Received September 15, 2003; Revised Manuscript Received November 13, 2003

ABSTRACT: Nitrite reductases found in plants, algae, and cyanobacteria catalyze the six-electron reduction of nitrite to ammonia with reduced ferredoxin serving as the electron donor. They contain one siroheme and one [4Fe-4S] cluster, acting as separate one-electron carriers. Nitrite is thought to bind to the siroheme and to remain bound until its complete reduction to ammonia. In the present work the enzyme catalytic cycle, with ferredoxin reduced by photosystem 1 as an electron donor, has been studied by EPR and laser flash absorption spectroscopy. Substrate depletion during enzyme turnover, driven by a series of laser flashes, has been demonstrated. A complex of ferrous siroheme with NO, formed by two-electron reduction of the enzyme complex with nitrite, has been shown to be an intermediate in the enzyme catalytic cycle. The same complex can be formed by incubation of free oxidized nitrite reductase with an excess of nitrite and ascorbate. Hydroxylamine, another putative intermediate in the reduction of nitrite catalyzed by nitrite reductase, was found to react with oxidized nitrite reductase to produce the same ferrous siroheme−NO complex, with a characteristic formation time of about 13 min. The rate-limiting step for this reaction is probably hydroxylamine binding to the enzyme, with the conversion of hydroxylamine to NO at the enzyme active site likely being much faster.

Inorganic nitrogen assimilation in oxygenic photosynthetic organisms involves several steps, including the six-electron reduction of nitrite to ammonia catalyzed by nitrite reductase, a reaction that uses reduced ferredoxin as the physiological electron donor (*1*). Ferredoxin-dependent nitrite reductases (EC 1.7.7.1) are 60−65 kDa proteins that are present both in photosynthetic tissues, where ferredoxin (Fd) is reduced by photosystem 1 (PS1),[1] and in nonphotosynthetic tissues, where Fd can be reduced by NADPH in a reaction catalyzed by ferredoxin−$NADP^+$ reductase (*1*). Ferredoxin-dependent nitrite reductases (NiR) have been purified from a number of photosynthetic organisms (*1*), including spinach (the enzyme used in this study). A complete amino acid sequence of spinach NiR has been derived from the gene sequence of the spinach chloroplast enzyme and the N-terminal amino acid sequence of the mature form of the protein (*2*).

The reduction of nitrite to ammonia requires six electrons, and no partially reduced intermediates released from the enzyme's active site have ever been observed during the catalytic process. As nitrite reductase has only one ferredoxin binding site [the enzyme has been shown to form an electrostatically stabilized 1:1 complex with Fd (*1*)] and the [2Fe-2S] cluster of ferredoxin can only donate a single electron at a time, the enzyme must somehow utilize its electron-carrying prosthetic groups to accumulate the electrons during the catalytic cycle. NiR is known to contain one siroheme (*3*) and one [4Fe-4S] cluster (*4*, *5*) as the only prosthetic groups (*1*). Although the X-ray structure of spinach nitrite reductase is not known, spectroscopic studies and sequence analogies indicate that the catalytic site of nitrite reductase is likely to be quite similar to that of the hemoprotein subunit of *Escherichia coli* sulfite reductase (SiR-HP), for which a high-resolution X-ray structure is available (*6*). In SiR-HP a sulfur atom from a cysteine residue is a common ligand both for the [4Fe-4S] cluster and for the siroheme iron (*6*). Despite being strongly coupled by the bridging ligand, the two prosthetic groups of spinach nitrite reductase act as independent one-electron carriers in oxidation−reduction titrations, with E_m values (at pH 7.0) of −365 mV for the [4Fe-4S] cluster and −290 mV for the siroheme (*7*). Electron transfer from the iron−sulfur cluster to the siroheme, i.e., in the thermodynamically favorable direction, has been shown to occur in spinach nitrite reductase (*7*).

NiR, as isolated, is fully oxidized, and the siroheme is in the high-spin ferric state. The reaction of oxidized NiR with its substrate, nitrite, leads to the formation of an EPR-silent oxidized NiR−NO_2^- complex (*8*). The siroheme in the spinach NiR complex with nitrite (as well as in the SiR−HP complex with sulfite) has been shown to remain oxidized and become low spin (*8*, *9*). The absence of an observable

† This work was funded, in part, by a grant (to D.B.K.) from the U.S. Department of Energy (DE-FG03-99ER20346). S.K. was supported by a long-term FEBS fellowship.

* To whom correspondence should be addressed. Phone: (+33) 169 08 98 67. Fax: (+33) 169 08 87 17. E-mail: setif@dsvidf.cea.fr.

‡ CEA Saclay.

§ Department of Chemistry and Biochemistry, Texas Tech University.

|| Center for Biotechnology and Genomics, Texas Tech University.

[1] Abbreviations: PS1, photosystem 1; Fd, ferredoxin; NiR, ferredoxin:nitrite oxidoreductase; EPR, electron paramagnetic resonance; oxyHb, oxyhemoglobin; metHb, methemoglobin.

10.1021/bi035662q CCC: $27.50 © 2004 American Chemical Society
Published on Web 12/16/2003

Scheme 1: Intermediates in the Catalytic Cycle of Nitrite Reductase

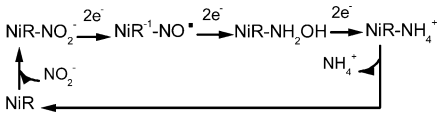

EPR signal from the resulting $S = {}^1/_2$ enzyme−substrate complex has been ascribed to *g*-strain (*8*). By analogy with *E. coli* sulfite reductase (*6*) and from model studies of hemoporphyrins in solution (*10*), nitrite is likely to bind to an axial position of the siroheme of the enzyme, with the nitrogen of nitrite acting as the sixth ligand for the heme iron.

A complex of NO with reduced siroheme, presumably formed after two-electron reduction of the oxidized enzyme with bound nitrite, has been characterized by electron paramagnetic resonance (EPR) spectroscopy *(4)*. This complex, with a characteristic axial EPR signal at $g_x = g_y = 2.06$ and $g_z = 2.007$, has been suggested to be an intermediate in nitrite reductase turnover (*4*, *11*). Its spectrum differs from those of ferroheme−NO complexes observed with other enzymes and displays closer resemblance to spectra of five-coordinated heme−NO complexes rather than to those containing six-coordinated iron (see, for example, refs *12* and *13*). This is probably due to the fact that, in most hemoproteins where complexes with NO have been studied, the heme is coordinated by a histidine at the axial position opposite from the substrate, while this axial ligand is likely to be a cysteine sulfur in the case of nitrite reductase.

Hydroxylamine (NH_2OH), formed from NO on reduction by three electrons, was proposed as a subsequent intermediate in nitrite reduction to ammonia catalyzed by NiR. Although many isolated nitrite reductases are able to convert hydroxylamine into ammonia (*14*, *15*), there is no definitive evidence that hydroxylamine serves as an intermediate in the reaction catalyzed by spinach nitrite reductase.

The supposed catalytic cycle of plant NiR, derived from these observations, is given in Scheme 1. Unambiguous evidence for the formation of these possible intermediates during enzyme turnover has not yet been obtained, and nothing is known about the reversibility or the kinetics of individual steps. It should also be pointed out that many studies on the enzyme catalytic cycle were carried out with nonphysiological electron donors and that no intermediates were detected in the few studies carried out with the physiological electron donor, ferredoxin (*15*). The present work was aimed at observing the complete enzyme turnover and at identifying the intermediates of the NiR catalytic cycle when ferredoxin, reduced by photosystem 1, serves as the electron donor.

MATERIALS AND METHODS

Materials. Spinach nitrite reductase was prepared using the procedure of Hirasawa et al. (*16*). The absorption spectrum of purified enzyme exhibits maxima at 278, 390, and 573 nm as previously reported (*9*, *14*). An absorption coefficient of 40000 M^{-1} cm^{-1} at 390 nm (*17*) was used to measure the enzyme concentration.

Photosystem 1 (PS1) reaction centers from the cyanobacterium *Synechocystis* sp. PCC 6803 were prepared as previously reported in ref *18*. *Synechocystis* PS1 was used, as it contains smaller amounts of chlorophyll than PS1 isolated from higher plants (which is an advantage in optical measurements). *Synechocystis* ferredoxin, overexpressed in *E. coli*, and plastocyanin (PCy), also from *Synechocystis* sp. PCC 6803, were used as electron donors for nitrite reductase and photosystem 1, respectively. Preliminary studies indicated that spinach nitrite reductase can be efficiently reduced by *Synechocystis* ferredoxin and that the steady-state kinetic parameters measured with *Synechocystis* ferredoxin as the electron donor for nitrite reduction are similar to those obtained with spinach ferredoxin. These observations are consistent with the fact that ferredoxin is highly conserved in all photosynthetic organisms and considerable sequence homology exists between the spinach and *Synechocystis* ferredoxins (*19*).

Flash-Induced NiR Reduction. The enzyme turnover was studied in a mixture containing PS1, Fd, plastocyanin, NiR, and nitrite. The sequence of electron transfer, PS1 → Fd → NiR → substrate, was triggered by a short saturating laser flash. The single flash caused a single charge separation in PS1 and formed an equal amount of free reduced Fd within less than 1 ms (*18*). The charge separation in PS1 includes the oxidation of the primary donor P700, which is a chlorophyll *a* dimer. $P700^+$ concentration was estimated from the flash-induced absorption changes at 820 nm assuming an absorption coefficient of 6500 M^{-1} cm^{-1} for $P700^+$ (*20*). Plastocyanin served as an electron donor for PS1, and an excess of ascorbate was used to reduce PCy. The kinetics of flash-induced PCy oxidation by PS1 from *Synechocystis* under similar experimental conditions has been investigated by Hervás et al. (*21*). Unless otherwise stated, experiments were carried out at pH 7.8 in buffer solution containing 20 mM Tricine, 30 mM NaCl, 0.03% *n*-dodecyl *β*-D-maltoside, and 5 mM $MgCl_2$ (standard solution). These conditions have been shown to be optimal for efficient interaction between *Synechocystis* PS1 and Fd (*18*). PS1-containing samples were prepared in low-intensity green light to avoid charge separation and electron transfer during the preparation.

Flash-induced absorption changes were recorded at room temperature using the apparatus previously described (*22*). Cuvettes with 1 mm path length were used. The flash repetition rate, unless otherwise stated, was 0.2 Hz. In the experiments on substrate depletion, samples in 1 mm path length optical cuvettes were exposed to multiple flashes using the same apparatus and, where indicated, subsequently transferred into EPR tubes and frozen in an ethanol bath. Single flashes given to EPR samples at room temperature were provided by a Nd:YAG laser (532 nm, 550 mJ, 8 ns) as previously described (*23*).

NiR Reduction by One or Two Electrons on Single Flash. The conditions for obtaining NiR reduction by one or two electrons per single flash were chosen on the basis of probability considerations. Previous experiments on flash-induced Fd reduction by PS1 (see, for example, ref *18*) have shown that, for a sample containing oxidized Fd and PS1 (with [Fd] ≥ [PS1]), a single flash causes charge separation in more than 95% of PS1 reaction centers, and an equal amount of reduced Fd is formed (so that finally the amount of Fd^- produced per flash approximately equals the PS1 concentration). If oxidized NiR is in large (3−5 times) excess over reduced Fd, then the probability that a given NiR molecule can be reduced by two different reduced Fds is

relatively low, as the probability that reduced Fd will bind to an oxidized NiR is much larger than the probability that it will bind to a reduced NiR. Thus, under these conditions, the main process will be single reduction of NiR. This probability consideration is based on the assumption that there is no specific process which would allow a second reduction to be unexpectedly favored (due to kinetic and/or energetic reasons) compared to the first reduction. No indication for such process has been reported in the literature.

When reduced Fd is present at a 2-fold excess over NiR, it can be supposed, from the same probability reasons, that most of NiR will be doubly reduced. To indicate that the main redox state of NiR after a single flash is given is assumed to be NiR^{-1}, under the condition that [PS1] $\ll$ [NiR], and NiR^{-2}, when [PS1] = 2[NiR], we refer to them hereafter as "single-electron reduction" and "two-electron reduction conditions", respectively.

EPR. X-band EPR spectra were recorded at 15 K on a Bruker ESP 300 spectrometer with an Oxford Instruments cryostat. EPR samples were frozen in darkness in an ethanol bath. The slow (i.e., time scales of minutes) kinetics of ferrous siroheme−NO complex formation were measured using the same sample that was frozen and thawed several times.

Oxyhemoglobin Assay. To check the possibility of NO formation from nitrite and ascorbate in solution, an oxyhemoglobin assay for nitric oxide was used. NO reacts stoichiometrically with oxyhemoglobin (oxyHb) to produce methemoglobin (metHb) and nitrate with a bimolecular rate constant of $(3-5) \times 10^7$ M^{-1} s^{-1} (*24*). The rate of metHb formation can be followed either by the shift in the heme Soret band absorbance maximum from 415 nm for oxyHb to 406 nm for metHb (*25*) or by the appearance of a high-spin metHb EPR signal around $g = 6$. The oxyHb stock solution (1.9 mM) was a kind gift of Dr. J. Santolini.

RESULTS AND DISCUSSION

Oxidized Nitrite Reductase and Its Reaction with Nitrite. The nitrite reductase samples used for this study exhibited an EPR signal with $g = 6.82$, 5.08, and 1.95 (data not shown), essentially identical to that reported previously (*26*). This signal arises from high-spin oxidized siroheme (*5*, *26*) and indicates that the siroheme of the isolated enzyme is fully oxidized. Fitting the temperature dependence of the NiR high-spin ferriheme EPR signal, using the formula of Janick and Siegel (*27*), gives a value of the axial zero-field splitting constant $D = 8 \pm 1.5$ cm^{-1}, similar to that reported for the *E. coli* sulfite reductase hemoprotein subunit (*27*). Estimation of the ratio of rhombic to axial zero-field splitting constants, *E*/*D*, using the formulation described by Palmer (*28*), gives a value of $E/D = 0.036$ for spinach nitrite reductase, a value close to that of 0.027, reported for *E. coli* sulfite reductase (*29*). The addition of nitrite to oxidized NiR causes a complete loss of the enzyme's EPR signal in less than 2 min, presumably due to the formation of the EPR-silent NiR−NO_2^- complex (*8*).

Fe^{2+} Siroheme−NO NiR Formation in the Presence of Ascorbate and Nitrite. The nitrite reductase Fe^{2+} siroheme−NO complex, first detected by its characteristic EPR signal by Aparicio et al. in studies of the spinach enzyme (*4*), was identified as a possible intermediate in the turnover studies

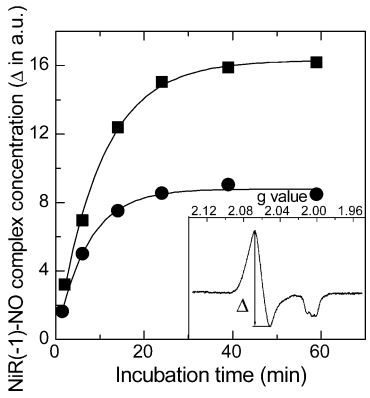

FIGURE 1: Kinetics of ferrous siroheme NiR−NO complex formation from nitrite and ascorbate. The sample contained 2 mM ascorbate, 3 mM $NaNO_2$, and 5 μM NiR (■) or 2.5 μM NiR (●). Each curve was obtained using a sample that was thawed, incubated, and refrozen between the measurements. The curves were fitted by the function $y = A[1 - \exp(-t/\tau)]$. The values of the parameters were $A = 16 \pm 2$, $\tau = 10.0 \pm 0.4$ min (■) and $A = 9 \pm 1$, $\tau = 7.1 \pm 0.4$ min (●). Inset: Spectrum of the nitrite reductase ferrous siroheme−NO complex. Nitrite reductase was frozen after incubation with 3 mM $NaNO_2$ and 2 mM ascorbate at room temperature for 30 min. Δ denotes the parameter used to estimate the concentration of the ferrous siroheme−NO complex. EPR measurement conditions: temperature, 15 K; microwave power, 0.2 mW; frequency, 9.4 GHz; modulation amplitude, 0.4 mT.

of the vegetable marrow enzyme by Cammack et al. (*11*). However, as no subsequent states in the turnover were detected in that study (*11*), the possibility that this complex is a "dead-end" product could not be completely excluded. The EPR spectrum of this complex of the spinach enzyme, obtained in our current study (Figure 1, inset, axial signal with $g_x = g_y = 2.06$ and $g_z = 2.007$), is in good agreement with those reported in previous studies (*11*, *30*, *31*).

We have found that a spectroscopically identical Fe^{2+} siroheme−NO complex of nitrite reductase can be formed in two different ways: (1) As will be shown below, this complex is formed during enzyme turnover. (2) Incubation of oxidized NiR with an excess of ascorbate and nitrite can produce the Fe^{2+} siroheme−NO complex in a process with a characteristic time of 10 ± 0.4 min (Figure 1). The amount of the complex formed by this second pathway depends linearly on NiR concentration (Figure 1).

However, neither the amount of the complex formed nor the rate of its formation changes when the nitrite concentration is decreased by a factor of 10, from 3 mM to 300 μM (data not shown). Although the formation of the NiR Fe^{2+} siroheme−NO complex on addition of nitrite and ascorbate to oxidized enzyme had previously been observed for vegetable marrow NiR (*30*), no mechanism for this reaction was proposed.

Two possible mechanisms for this formation can be suggested. First, NO could be formed from nitrite in solution, either without any reductant or from nitrite reduction by ascorbate. The NiR siroheme also could be reduced by ascorbate either through electron transport from the [4Fe-4S] cluster or directly. NO would then be trapped by the reduced enzyme to form a NiR(−1)−NO complex. The second possibility is that the reaction between ascorbate, nitrite, and siroheme occurs at the enzyme catalytic site.

To distinguish between these two possible mechanisms of NO formation, 5 μM NiR was incubated with a large

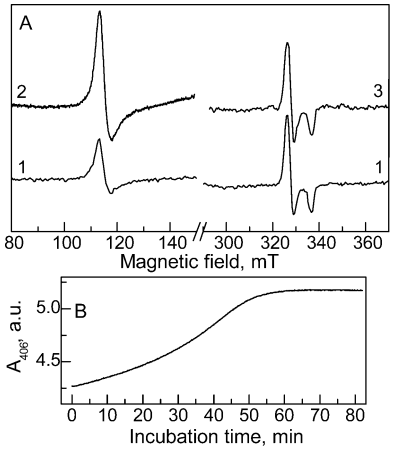

FIGURE 2: NiR(−1)−NO complex formation on NiR incubation with nitrite and ascorbate in the presence of oxyHb. (A) Samples 1 (assayed sample) and 3 (control sample) contained 2 mM ascorbate, 3 mM $NaNO_2$, and 5 μM NiR. OxyHb was added to sample 1 to a final concentration of 15 μM in three equal portions (after 0, 10, and 20 min of incubation) to account for oxyHb oxidation by nitrite and to ensure that oxyHb is always present in the sample. Sample 3 contained no oxyHb. Both samples were frozen after 30 min incubation at room temperature. Sample 2: 15 μM oxyHb was incubated with 3 mM nitrite in 20 mM Tricine/30 mM NaCl until the absorption at 406 nm became maximal and then frozen. EPR measurement conditions: temperature, 15 K; microwave power, 2 mW; frequency, 9.4 GHz; modulation amplitude, 1 mT. (B) Kinetics of oxyHb oxidation by nitrite. The sample contained 5 μM oxyHb and 3 mM nitrite in 20 mM Tricine/30 mM NaCl.

excess of nitrite and ascorbate (the same conditions as in Figure 1, squares) in the presence of 15 μM oxyHb. If NO is formed according to the first of the suggested mechanisms (i.e., formed in solution and then bound to reduced NiR), it would be trapped by oxyHb, as the bimolecular constant of oxyHb oxidation by nitric oxide is very high [$(3-5) \times 10^7$ $M^{-1}s^{-1}$ (*24*)]. The competition with oxyHb would diminish the rate of NiR(−1)−NO formation, and metHb resulting from oxyHb reaction with nitric oxide could be quantitated by its EPR signal.

The results of the oxyHb assay of NiR(−1)−NO complex formation on NiR incubation with nitrite and ascorbate are shown in Figure 2. The amount of the NiR(−1)−NO complex in the oxyHb-containing sample after 30 min incubation (Figure 2A, curve 1) is exactly the same as in the control sample containing no oxyHb (Figure 2A, curve 3) and corresponds to more than 90% of total NiR concentration (see Figure 1). The small amount of metHb observed in the presence of nitrite and ascorbate (Figure 2A, curve 1) is due to slow oxyHb oxidation by nitrite (*32*) and does not exceed the amount formed on incubation of oxyHb, at the same concentration, with nitrite alone (not shown). The kinetics of this reaction are shown in Figure 2B. The comparison of metHb concentration in the NiR sample (Figure 2A, curve 1) to the reference sample corresponding to full oxidation of 15 μM oxyHb to metHb (Figure 2A, curve 2) shows that, by the end of incubation, the NiR sample contains about 9 μM oxyHb (6 μM metHb being present out of a total concentration of 15 μM Hb), and thus oxyHb is present in excess over NiR during the incubation. The fact that competition with oxyHb does not affect the amount of the NiR(−1)−NO complex shows that no free NO is trapped in the solution and NO is formed in the enzyme catalytic site where it cannot react with oxyHb. The possibility that NO, formed in solution, subsequently diffuses to the enzyme's active site can thus be eliminated, and we conclude that the NiR(−1)−NO complex arises from reactions that take place at the enzyme's active site. Our data allow us to examine the possible mechanism for these reactions in more detail.

As the high-spin ferric siroheme EPR signal disappears after a 2 min incubation of enzyme with nitrite (see above), it seems feasible that nitrite first binds to the siroheme and then ascorbate reduces both the heme and the nitrite at the catalytic site, forming the Fe^{2+} siroheme−NO complex. This possibility is consistent with our observation that the rate of NiR(−1)−NO complex formation is independent of the concentration of nitrite in solution, as only the nitrite bound to the heme can take part in the reaction. As expected from the known E_m values for ascorbate and the siroheme of NiR, ascorbate at the concentrations used in our experiments is not able to reduce the siroheme (it was still in the high-spin ferric state even after 1 h incubation of nitrite reductase with ascorbate; data not shown). Thus during its reaction with the NiR−NO_2^- complex, ascorbate most likely first donates an electron to nitrite, converting it into NO, with the resulting reactive ascorbate radical then reducing the siroheme. The participation of monodehydroascorbate in the reaction is supported by the finding that the sample containing NiR and an excess of nitrite and ascorbate (the same conditions as in Figure 1, squares) during formation of the Fe^{2+} siroheme−NO complex contains about 75% more of monodehydroascorbate radical than the analogous sample without NiR (as detected by room temperature EPR; data not shown). The fact that addition of NiR to a solution containing nitrite and ascorbate, both in large excess compared to NiR (600- and 400-fold, respectively), nearly doubles the amount of ascorbate radical suggests that the additional radical is formed in a NiR-initiated reaction. Reduction of enzyme-bound nitrite by ascorbate could be facilitated by a change in the redox potential of nitrite due to interaction with the heme and/or with surrounding positively charged amino acids. Enzymes such as cytochrome *c* nitrite reductase utilize positively charged amino acids to accommodate the negatively charged oxygens of the nitrite molecule (*33*). Similar reactions have also been observed with other hemes. For example, incubation with nitrite and excess ascorbate is one of the methods routinely used to form ferroheme complexes with nitric oxide in hemoproteins (*12*).

The maximal signal of the Fe^{2+} siroheme−NO complex observed in our experiments, delineated by the closed squares in Figure 1 (at an incubation time of 60 min or more), has been taken to represent the signal amplitude arising from the conversion of all of the NiR present to the Fe^{2+} siroheme−NO state and has been used to estimate the concentration of this state observed in other experiments.

Fe^{2+} Siroheme−NO NiR as an Intermediate in the Catalytic Cycle. As mentioned above, the Fe^{2+} siroheme−NO complex can also be produced on reduction of the NiR complex with nitrite by reduced Fd. We have tried to determine whether the formation of this complex from the oxidized NiR−NO_2^- complex is a single or a two-electron reduction reaction.

Figure 3 shows a comparison of the signal observed after excitation of a mixed PCy-PS1-Fd-NiR-NO_2^- sample by a

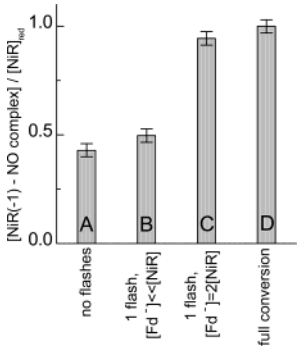

FIGURE 3: Flash-induced formation of the NiR(−1)−NO complex in single-electron and two-electron reduction conditions. (B) NiR(−1)−NO complex signal after a single flash given after 4 min incubation to a sample containing 6 μM PS1, 3 μM PCy, 6 μM Fd, 14.6 μM NiR, 3 mM $NaNO_2$, and 2 mM ascorbate in standard solution (single-electron reduction conditions), which was mixed rapidly in low-intensity green light. (C) NiR−NO complex signal after a single flash given after 4 min incubation to a sample containing 10 μM PS1, 10 μM PCy, 15 μM Fd, 5 μM NiR, 3 mM $NaNO_2$, and 2 mM ascorbate in standard solution (two-electron reduction conditions), which was mixed rapidly in low-intensity green light. (A) and (D) correspond to the amount of NiR(−1)−NO complex formed with 5 μM NiR in the presence of 3 mM $NaNO_2$ and 2 mM ascorbate (same conditions as for Figure 1, squares) for incubation times of 4 min (A) and 60 min (D). $[NiR]_{red}$ denotes the concentration of NiR that has been reduced by Fd^-; it is taken to be equal to full [NiR] for two-electron reduction and to [PS1] in single-electron reduction conditions (see Materials and Methods).

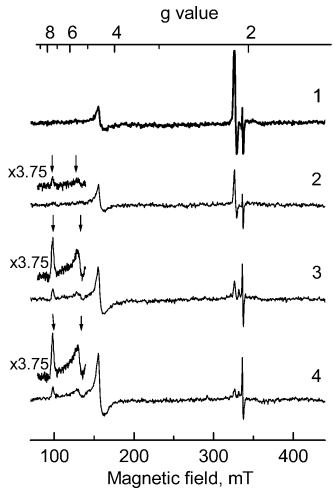

FIGURE 4: Nitrite reductase turnover in the presence of a 2-fold excess of reduced ferredoxin analyzed by low-temperature EPR spectroscopy. The sample contained 10 μM PS1, 10 μM PCy, 15 μM Fd, 5 μM NiR, 50 μM $NaNO_2$, and 2 mM ascorbate in standard solution. (1) The sample was mixed rapidly in low-intensity green light and frozen after a single saturated laser flash. (2) An identical sample frozen after 60 laser flashes. (3) 96 laser flashes were given to the mixture (1) and then the sample was frozen. (4) Sample 3 was thawed, illuminated by 48 flashes, and refrozen. The high-spin ferric siroheme signal is marked by arrows. The $g = 2$ radical signal comes from $P700^+$. EPR measurement conditions: temperature, 15 K; microwave power, 2 mW; frequency, 9.4 GHz; modulation amplitude, 1 mT.

single flash to the maximum signal amplitude observed after long NiR incubation with excess nitrite and ascorbate (Figure 3D). We first used the two-electron reduction conditions, i.e., a 2-fold excess of PS1 compared to NiR (see Materials and Methods). When flash excitation was given to such a sample, one that showed only a partial formation of Fe^{2+} siroheme−NO signal before the flash (Figure 3A), the signal amplitude became maximal (Figure 3C) with EPR features that are identical to the signal produced in the dark in the presence of nitrite and ascorbate. Therefore, we can conclude that donation of two electrons to spinach NiR in the presence of nitrite efficiently converts the enzyme to the Fe^{2+} siroheme−NO state. We also tested single-electron reduction conditions, i.e., when a single flash was given to a sample containing an excess of NiR over PS1 (Figure 3B). Under these conditions, almost no Fe^{2+} siroheme−NO was photoproduced beyond the amount formed from ascorbate and nitrite prior to illumination (Figure 3A). These results indicate that, during enzyme turnover, formation of the Fe^{2+} siroheme−NO complex requires reduction of the NiR complex with nitrite by two electrons and that reduction by one electron does not suffice.

Enzyme Turnover Driven by Reduced Fd and Substrate Depletion by Two-Electron Reduction. Clear evidence for enzyme turnover under the conditions used in this investigation of spinach nitrite reductase would come from a demonstration of nitrite disappearance. If this were to occur, the Fe^{2+} siroheme−NO complex should vanish and free oxidized enzyme should appear, leading to changes both in EPR signals and in flash-induced absorption kinetics.

Figure 4 shows, using EPR detection under conditions of two-electron reduction ([PS1] = 2[NiR]), that nitrite depletion does indeed occur during a train of short saturating laser flashes. After a single flash, only the Fe^{2+} siroheme−NO signal is visible (Figure 4, curve 1). A comparison of the amplitude of this EPR signal to the maximal ferroheme−NO signal observed after incubation of a sample of identical NiR concentration with nitrite and ascorbate (Figure 1) shows that 88% of the enzyme is in the NiR(−1)−NO state. The magnitude of the Fe^{2+} siroheme−NO EPR signal decreases significantly after 60 flashes, and an EPR signal characteristic of the unliganded high-spin ferric siroheme appears (Figure 4, curve 2). This indicates that as a result of illumination by this series of flashes the concentration of nitrite in the sample has become comparable to that of the enzyme. If this were not the case, nitrite would bind to free NiR, forming the EPR-silent enzyme−substrate complex and no EPR signal characteristic of free NiR would be visible. When 96 flashes were given to the sample, the EPR signal attributable to free oxidized NiR became even more apparent and corresponded to about 68% of the total enzyme concentration (Figure 4, curve 3). Illumination of the same sample by an additional 48 flashes (for a total of 144 flashes) made the Fe^{2+} siroheme−NO signal disappear almost completely, with approximately 88% of the total enzyme present in the oxidized and unliganded form (Figure 4, curve 4).

The substrate depletion can also be followed by flash-induced absorption changes. The difference in the flash-induced absorption changes between the free enzyme and the enzyme−substrate complex is most obvious in the near-infrared region, where Fd reduction by PS1 iron−sulfur clusters and Fd^- reoxidation does not contribute (*18*). Figure 5 shows flash-induced absorption changes measured at 950 nm of a control sample (neither NiR nor nitrite present, curve 1), free enzyme (NiR in the absence of substrate, curve 4), and the enzyme−substrate complex (NiR in the presence of nitrite, curves 2 and 3) under two-electron reduction conditions (2-fold excess of PS1 over NiR). To compare the four

different curves shown in Figure 5, it has been assumed that PS1 oxidation and reduction are not affected by soluble acceptors of electrons from ferredoxin and thus contribute equally to the absorption transients obtained with control and with the NiR-containing samples. As there is no contribution from Fd reduction or reoxidation at 950 nm, the difference between the NiR-containing and the control samples represents the absorption changes due to NiR or NiR−substrate complex reduction.

The absorption changes in the control sample (Figure 5, curve 1) are ascribed to P700 photooxidation (the initial rise), which is followed by $P700^+$ reduction by PCy. The NiR-containing sample (no substrate) shows an absorption increase at 950 nm upon reduction (Figure 5, curve 4), when compared to control (curve 1). The published reduced *minus* oxidized difference spectra of free NiR show an increase of absorption in the near-infrared region (see ref *7* for a difference spectrum arising from the full, two-electron reduction and ref *34* for difference spectra arising from the separate reductions caused by the first and second electrons), although the absorption difference at 950 nm was not reported. The two-electron reduction of the enzyme−substrate complex leads to an initial absorption decrease and a subsequent increase at 950 nm (compare curve 2 to curve 1). However, after 4 min of continuous preillumination, the flash-induced absorption kinetics of the complex, monitored at 950 nm, essentially revert to those observed for the free enzyme (Figure 5, curve 3).

This observation suggests that the substrate is consumed during continuous illumination so that no new enzyme−substrate complex can be formed in the sample. Indeed, the change in the form of the flash-induced absorption kinetics from the initial decay to an initial rise (Figure 5: the transition from curve 2 to curve 3) coincides with the appearance of the free NiR signal in the EPR spectrum of the sample (Figure 4, curve 2). Thus the flash-induced absorption changes in the near-infrared region can be used as an indication of the substrate depletion by flashes.

To estimate the efficiency of flash-driven enzyme turnover with about a 2-fold excess of reduced ferredoxin, we have determined the minimum number of flashes necessary for the appearance of the free oxidized NiR signal. Then the efficiency can be estimated as

$$\frac{N_{\min}}{N_{\text{measured}}} \times 100\% \qquad (1)$$

where $N_{\min} = 6[NO_2^-]_{\text{consumed}}/[Fd^-]$, $[NO_2^-]_{\text{consumed}} = [NO_2^-]_{\text{initial}}$, and $[Fd^-] = [P700^+]$.

N_{measured} was found to be about 60 (Figure 4), corresponding to an enzyme efficiency of 50 ± 2%.

Several factors could have caused an underestimation of the efficiency of nitrite reduction in our sample. One possibility is that a portion of the flash-reduced Fd^- is reoxidized by dissolved oxygen between the flashes before it can donate an electron to NiR. Another possible cause of underestimation of NiR efficiency could be NiR reoxidation; i.e., unstable intermediates in the NiR catalytic cycle may be partially reoxidized between the flashes. However, the changes in experimental conditions designed to diminish the influence of these factors did not lead to an increase of nitrite reduction efficiency calculated according to eq 1. The amount

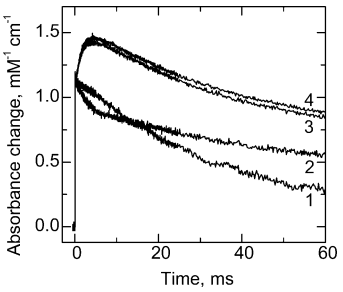

FIGURE 5: Flash-induced absorption changes measured at 950 nm under two-electron reduction conditions ([PS1] = 2[NiR], when NiR is present): (1) no NiR, no NO_2^-, (4) 2 μM NiR, no NO_2^- after 4 min of illumination, (2) 2 μM NiR, 100 μM NO_2^- before and (3) after 4 min of illumination. All of the samples contained 4 μM PS1, 5 μM PCy, 6 μM Fd, and 2 mM ascorbate in standard solution.

of ferredoxin or NiR that is reoxidized between the flashes would be expected to decrease if the interval between the flashes were shortened. Nevertheless, the efficiency of nitrite consumption under two-electron reduction conditions was found to be the same for intervals between the flashes ranging from 1 to 5 s (not shown). Deoxygenation of the sample with a 2-fold excess of reduced ferredoxin (same conditions as for Figure 4) by several cycles of degassing and pumping with argon also did not decrease the number of flashes required to observe the EPR signal characteristic of free oxidized NiR. It thus appears that the reoxidation of Fd^- by dissolved oxygen does not diminish the NiR efficiency in our system. The reoxidation of partially reduced intermediates in NiR turnover either does not affect the efficiency of nitrite depletion by flashes or occurs in less than 1 s and thus is the same for the intervals between the flashes larger than 1 s that we have studied.

Hydroxylamine Reaction with Nitrite Reductase. To investigate the later intermediates of the enzyme catalytic cycle, the reaction of NiR with hydroxylamine was studied. The appearance of the Fe^{2+} siroheme−NO signal when oxidized NiR was mixed with hydroxylamine was first observed by Lancaster et al. (*5*), but the kinetic characteristics of this reaction were not reported. Vega and Kamin (*14*) reported that the reaction of hydroxylamine with oxidized NiR took about 20 min to go to completion, but this study did not identify the product of that reaction. The redox state of the enzyme cofactors in the presence of hydroxylamine is not known, but it is possible that the intermediate in the enzyme turnover is the $[4Fe\text{-}4S]_{ox}$−Fe^{3+} siroheme−NH_2OH state, as has been suggested for cytochrome *c* nitrite reductase (*33*, *35*). The reduction of hydroxylamine to ammonia requires two electrons, and as NiR seems to be capable of carrying out two-electron transfer steps (see above), a complex of the oxidized enzyme with hydroxylamine could, in principle, represent a mechanistically important intermediate in the catalytic cycle.

The kinetics of NO formation from hydroxylamine, catalyzed by NiR, are shown in Figure 6. The absorption difference spectrum of NiR in the presence of an excess of hydroxylamine (28 min incubation *minus* 2 min incubation) has a maximum at 588 nm and minima at 490 and 696 nm (Figure 6, inset), in good agreement with the spectrum previously measured by Vega and Kamin (*14*). The time course for changes in the NiR absorption spectrum after

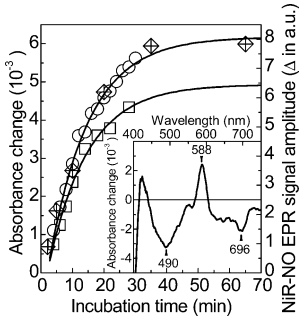

FIGURE 6: Kinetics of NiR(−1)−NO formation from NiR and NH_2OH from absorption data. 10 μM nitrite reductase was mixed with 10 mM NH_2OH in 20 mM Tricine buffer (pH 7.8), and absorption spectra were measured after incubation at room temperature. The spectrum 2 min after mixing was taken as a reference. (○) $\Delta A_{588-490}$, $\tau = 12.8 \pm 0.8$ min; (□) $\Delta A_{588-696}$, $\tau = 13 \pm 1$ min. The amplitude of the NiR(−1)−NO EPR signal is given for comparison (crossed ◇). Inset: Difference of absorption spectra of the same sample after 28 and 2 min of incubation.

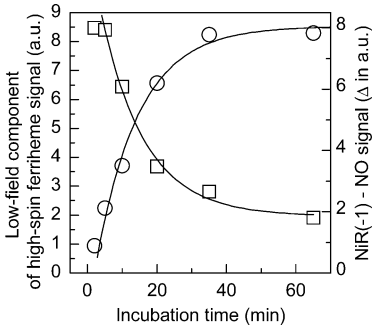

FIGURE 7: Reaction of oxidized nitrite reductase with hydroxylamine: comparative kinetics of the free NiR signal disappearance and NiR(−1)−NO formation. 10 μM nitrite reductase was mixed with 10 mM NH_2OH in 20 mM Tricine and frozen after 2−65 min of incubation at room temperature. (○) Amplitude of the ferrous siroheme−NO signal. (□) Amplitude of the high-spin ferric siroheme signal ($g = 6.8$ feature). The NO appearance curve (●) was fitted by the function $y = A[1 - \exp[-(t - t_0)/\tau]]$, $\tau = 12.3 \pm 1.4$ min, and $t_0 = 2$ min and the high-spin ferric siroheme disappearance (■) by single-exponential decay $y = A \exp[-(t - t_0)/\tau)]$, $\tau = 12.5 \pm 1.8$ min, and $t_0 = 2$ min. The experiment was performed on a similar sample that was thawed, incubated, and refrozen between the measurements. EPR measurement conditions: temperature, 15 K; microwave power, 2 mW; frequency, 9.4 GHz; modulation amplitude, 1 mT; receiver gain, 10^5; eight scans.

incubation with hydroxylamine shows no indication of intermediate states. The shape of the difference spectrum observed (Figure 6, inset) is independent of the time at which it was measured. The half-time for the appearance of the species responsible for this difference spectrum is 13 ± 1 min (Figure 6).

The kinetics of NO formation from hydroxylamine, catalyzed by spinach NiR, were found to be the same under aerobic and anaerobic (in the sample deoxygenated by several cycles of pumping and argon flushing) conditions (not shown). This result suggests that either the hydroxylamine oxidation uses an electron acceptor other than dissolved oxygen or that the oxygen amount left after the deoxygenation is sufficient to drive this reaction.

The fact that the NiR(−1)−NO EPR signal and the difference spectrum of the inset to Figure 6 appear with the same kinetics strongly suggests that this difference spectrum results from Fe^{2+} siroheme−NO formation.

One may ask whether the $NiR_{ox} + NH_2OH \rightarrow Fe^{2+}$ siroheme−NO reaction described above represents the reversal of a normal step in the enzyme catalytic cycle. If so, why are intermediate states of this reaction (for example, the NH_2OH complex with ferric siroheme) not seen? There are at least two possible explanations for the lack of observed intermediates:

(1) The NiR complex with hydroxylamine observed when the oxidized enzyme is mixed with NH_2OH is not a true intermediate, and thus the observed reaction does not represent a real reversal of a step in the enzyme's catalytic cycle. For example, Fe^{2+} siroheme−NO production has been demonstrated to occur as a result of tetraphenylporphyrin-mediated disproportionation of two NH_2OH molecules, bound on different sides of the heme, to NO and ammonia in solution (*36*). However, if the structure of the NiR catalytic site strongly resembles that of *E. coli* SiR-HP (as appears to be the case), the binding of two NH_2OH molecules to NiR seems very unlikely because of the presence of one axial cysteine sulfur ligand. Therefore, it appears unlikely that this reaction can occur when NiR is incubated with hydroxylamine.

(2) The binding of hydroxylamine to NiR is slow, while the back-reaction itself is much faster, and thus the rate we observe is in fact the rate of hydroxylamine binding. Such a slow binding could perhaps be caused by electrostatic repulsion between the protons of hydroxylamine and some basic groups coordinating nitrite in the binding site.

The second possibility is supported by the following observation. During the first minutes of the reaction, while the amount of the Fe^{2+} siroheme−NO complex observed is still small, a portion of the NiR siroheme is still present as an oxidized high-spin species, exhibiting exactly the same EPR signal as the one observed for the free enzyme. This observation strongly suggests that not all of the NiR has bound hydroxylamine. Figure 7 shows that the kinetics observed for the loss of the high-spin ferric siroheme EPR signal and the appearance of the ferroheme−NO EPR signal are identical. Both show the same characteristic time of about 13 min. As in the case of optical difference spectra (see above), there was no evidence for an intermediate between free oxidized NiR and the ferroheme−NO NiR complex. Thus it seems very likely that the hydroxylamine reaction with oxidized nitrite reductase is binding-limited. It should be noted that our data do not allow us to conclude unambiguously that NO reduction to hydroxylamine during NiR turnover, if it occurs, and the oxidation of hydroxylamine to NO that we observe follow the same pathway. It is possible that the forward reaction proceeds through a relatively stable intermediate, preventing the loss of two electrons and the return to NO, while this intermediate is bypassed during hydroxylamine oxidation.

CONCLUSIONS

Figure 8 shows the catalytic cycle of plant nitrite reductase proposed on the basis of previous works and the results of the present study. Oxidized unliganded NiR binds nitrite to form an EPR-silent enzyme−substrate complex. The reduction of this complex by two electrons leads to the formation of the Fe^{2+} siroheme−NO state with a characteristic EPR signal. Janick et al. (*37*) have shown that this state is the

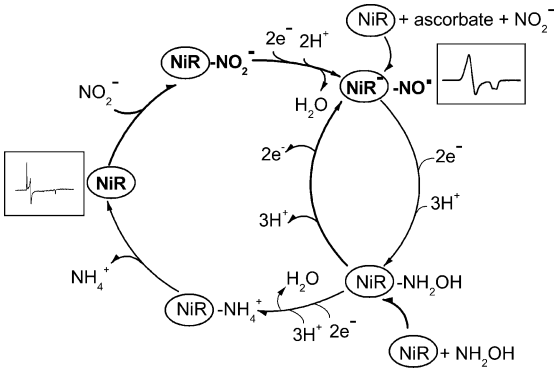

FIGURE 8: Catalytic cycle of ferredoxin-dependent nitrite reductase.

most prominent and stable intermediate observed during photoinduced nitrite reduction by *E. coli* sulfite reductase (nitrite is an alternative substrate for this enzyme) with deazariboflavin as an electron donor. The same complex can be formed during enzyme incubation with ascorbate and nitrite. One may hypothesize that such a complex could also form in the stromal space of chloroplasts, where the ascorbate concentration is quite high [12−25 mM (*38*)], but the extent of this reaction would also depend on the concentration of free nitrite in the stroma.

Oxidized NiR was also found to react with hydroxylamine to produce the same ferrous siroheme−NO complex formed by incubation of the enzyme with nitrite and a reductant. Our data strongly suggest that the rate-limiting step in the reaction of NiR with hydroxylamine is the hydroxylamine-binding step. It appears that the enzyme complex with hydroxylamine, $[Fe_4S_4]_{ox}$−Fe^{3+} siroheme−NH_2OH, represents a branching point in the enzyme catalytic cycle from which, in the absence of reductant, the enzyme returns to the Fe^{2+} siroheme−NO state, while it may proceed to the final product in the presence of reductant. However, as all of the intermediates following NO in the catalytic cycle are EPR silent, methods other than EPR spectroscopy will be needed to provide additional information about the nature of this branching point.

ACKNOWLEDGMENT

We thank Dr. Miruna Roman for help and guidance in the absorption spectra measurements and Dr. Tony Mattioli for valuable discussions. We are grateful to Dr. A. Díaz-Quintana for the gift of *Synechocystis* plastocyanin and to Dr. J. Santolini for the gift of oxyHb. We also thank Véronique Mary for skillful technical assistance.

REFERENCES

1. Knaff, D. B., and Hirasawa M. (1991) *Biochim. Biophys. Acta 1056*, 93−125.
2. Back, E., Burkhart, W., Moyer, M., Privalle, L., and Rothstein, S. (1988) *Mol. Gen. Genet. 212*, 20−26.
3. Murphy, M. J., Siegel, L. W., Tove, S. R., and Kamin, H. (1974) *Proc. Natl. Acad. Sci. U.S.A. 71*, 612−616.
4. Aparicio, P. J., Knaff, D. B., and Malkin, R. (1975) *Arch. Biochem. Biophys. 169*, 102−107.
5. Lancaster, J. R., Vega, J. M., Kamin, H., Orme-Johnson, N. R., Orme-Johnson, W. H., Krueger, R. J., and Siegel, L. M. (1979) *J. Biol. Chem. 254*, 1268−1272.
6. Crane, B. R., Siegel, L. M., and Getzoff, E. D. (1997) *Biochemistry 36*, 12120−12137.
7. Hirasawa, M., Tollin, G., Salamon, Z., and Knaff, D. B. (1994) *Biochim. Biophys. Acta 1185*, 336−345.
8. Young, L. J., and Siegel, L. M. (1988) *Biochemistry 27*, 2790−2800.
9. Day, E. P., Peterson, J., Bonvoisin, J. J., Young, L. J., Wilkerson, J. O., and Siegel, L. M. (1988) *Biochemistry 27*, 2126−2132.
10. Fernandes, J. B., Feng, D. W., Chang, A., Keyser, A., and Ryan, M. D. (1986) *Inorg. Chem. 25*, 2606−2610.
11. Cammack, R., Hucklesby, D. P., and Hewitt, E. J. (1978) *Biochem. J. 171*, 519−526.
12. Morse, R. H., and Chan, S. I. (1980) *J. Biol. Chem. 255*, 7876−7882.
13. Henry, Y., Ducrocq, C., Drapier, J.-C., Servent, D., Pellat, C., and Guissani, A. (1991) *Eur. Biophys. J. 20*, 1−15.
14. Vega, J. M., and Kamin, H. (1977) *J. Biol. Chem. 252*, 896−909.
15. Hucklesby, D. P., and Hewitt, E. J. (1970) *Biochem. J. 119*, 615−627.
16. Hirasawa, M., Fukushima, K., Tamura, G., and Knaff, D. B. (1984) *Biochim. Biophys. Acta 791*, 145−154.
17. Bellissimo, D. B., and Privalle, L. S. (1995) *Arch. Biochem. Biophys. 323*, 155−163.
18. Sétif, P., and Bottin, H. (1995) *Biochemistry 34*, 9059−9070.
19. Matsubara, T., and Hase, T. (1983) in *Nucleic Acids in Plant Systematics* (Jensen, U., and Fairbrothers, D. E., Eds.) pp 168−181, Springer-Verlag, Berlin.
20. Mathis, P., and Sétif, P. (1981) *Isr. J. Chem. 21*, 316−320.
21. Hervás, M., Ortega, J. M., Navarro, J. A., De la Rosa, M. A., and Bottin, H. (1994) *Biochim. Biophys. Acta 1184*, 235−241.
22. Sétif, P., and Bottin, H. (1994) *Biochemistry 33*, 8495−8504.
23. Boussac, A., Sugiura, M., Inoue, Y., and Rutherford, A. W. (2000) *Biochemistry 39*, 13788−13799.
24. Eich, R. F., Li, T., Lemon, D. D., Doherty, D. H., Curry, S. R., Aitken, J. F., Mathews, A. J., Smith, R. D., Phillips, G. N., and Olson, J. S. (1996) *Biochemistry 35*, 6976−6953.
25. Feelisch, M., Kubitzek, D., and Werrigloer, J. (1996) The oxyhemoglobin assay, in *Methods in nitric oxide research* (Feelisch, M., and Stamler, J. S., Eds.) Wiley, Chichester.
26. Hirasawa, M., Shaw, R. W., Palmer, G., and Knaff, D. B. (1987) *J. Biol. Chem. 262*, 12428−12433.
27. Janick, P. A., and Siegel, L. M. (1982) *Biochemistry 21*, 3538−3547.
28. Palmer, G. (1985) *Biochem. Soc. Trans. 13*, 548−560.
29. Christner, J. A., Münck, E., Janick, P. A., and Siegel, L. M. (1981) *J. Biol. Chem. 256*, 2098−2101.
30. Fry, I. V., Cammack, R., Hucklesby, D. P., and Hewitt, E. J. (1980) *FEBS Lett. 111*, 377−380.
31. Cammack, R., and Fry, I. V. (1980) *Biochem. Soc. Trans. 8*, 642.
32. Spagnuolo, C., Rinelli, P., Coletta, M., Chiancone, E., and Ascoli, F. (1987) *Biochim. Biophys. Acta 911*, 59−65.
33. Einsle, O., Messerschmidt, A., Stach, P., Bourenkov, G. P., Bartunik, H. D., Huber, R., and Kroneck, P. M. H. (1999) *Nature 400*, 476−480.
34. Wilkerson, J. O., Janick, P. A., and Siegel, L. M. (1983) *Biochemistry 22*, 5048−5054.
35. Einsle, O., Messerschmidt, A., Huber, R., Kroneck, P. M., and Neese, F. (2002) *J. Am. Chem. Soc. 124*, 11737−11745.
36. Choi, I.-K., Liu, Y., Wei, Z., and Ryan, M. D. (1997) *Inorg. Chem. 36*, 3113−3118.
37. Janick, P. A., Rueger, D. C., Krueger, R. J., Barber, M. J., and Siegel, L. M. (1983) *Biochemistry 22*, 396−408.
38. Foyer, C., Rowell, J., and Walker, D. (1983) *Planta 157*, 239−244.

BI035662Q